MODAL SURVEY OF ETM-3, A 5-SEGMENT DERIVATIVE OF THE SPACE SHUTTLE SOLID ROCKET BOOSTER

D. Nielsen*, J. Townsend†, K. Kappus‡, T. Driskill§, I. Torres**, R. Parks††

ABSTRACT

The complex interactions between internal motor generated pressure oscillations and motor structural vibration modes associated with the static test configuration of a Reusable Solid Rocket Motor have potential to generate significant dynamic thrust loads in the 5-segment configuration (Engineering Test Motor 3). Finite element model load predictions for worst-case conditions were generated based on extrapolation of a previously correlated 4-segment motor model. A modal survey was performed on the largest rocket motor to date, Engineering Test Motor #3 (ETM-3), to provide data for finite element model correlation and validation of model generated design loads. The modal survey preparation included pre-test analyses to determine an efficient analysis set selection using the Effective Independence Method and test simulations to assure critical test stand component loads did not exceed design limits. Historical Reusable Solid Rocket Motor modal testing, ETM-3 test analysis model development and pre-test loads analyses, as well as test execution, and a comparison of results to pre-test predictions are discussed.

INTRODUCTION

For many years modal testing has been the primary engineering tool used to determine the dynamic characteristics of aerospace structures. Modal testing technology has advanced rapidly with the advancement of computers and digital data acquisition systems. Today's testing techniques and analysis tools allow the engineer to verify his analytical math models in a very short time and cost efficient manner. This paper details the modal testing program completed by a NASA and ATK Thiokol joint engineering team on an experimental five-segment Solid Rocket Motor, known as Engineering Test Motor #3 (ETM-3).

This paper begins with a description of the ETM-3 motor and Thiokol's T-97 test stand facility. Synopsis on the modal test history of the Reusable Solid Rocket Motor (RSRM) is given along with a motivation for performing the ETM-3 modal test. It then examines the development details of the Test Analysis Model (TAM) in terms of target mode selection and pre-test analysis. The selection of accelerometer locations for the modal test using an analysis method known as the Effective Independence Method is discussed. A parameter sensitivity study is presented that identifies the primary contributors to test stand dynamic loading. Also, the paper gives a summary of the modal testing program along with modal survey test results. Modal test frequencies, dynamic mode shapes, and system damping values are highlighted. Included are insights into the importance of modal testing for validation purposes, and brief discussions of the ETM-3 performance relative to predictions. The paper concludes with a justification for completing the ETM-3 test fire, a post-test review and lessons learned section as well as an outline of future work.

Motor Description

The ETM-3 test motor consisted of five standard weight (case material thickness) segments each approximately 320 inches in length and weighing approximately 300,000 lbs. This configuration gave ETM-3 a total motor length of over 1840 inches and a weight of approximately 1.6 Mlbf, as compared to the current RSRM motor design for the Space Shuttle which utilizes four segments (both standard and lightweight mix) for a motor length and weight of approximately 1520 inches and 1.3 Mlbf, respectively. A pictorial of the ETM-3 motor is given in Figure 1, and major differences between the ETM-3 and RSRM

* Technical Manager, ATK Thiokol Inc., Design & Analysis, Brigham City, UT
† Aerospace Engineer, NASA/Marshall Space Flight Center, Structural Dynamics Lab, Huntsville, AL.
‡ Dynamic Test Engineer, NASA/Marshall Space Flight Center, Modal and Control Dynamics Team, Huntsville, AL.
§ Dynamic Test Engineer, NASA/Marshall Space Flight Center, Modal and Control Dynamics Team, Huntsville, AL.
** Aerospace Engineer, NASA/Marshall Space Flight Center, Structural Dynamics Lab, Huntsville, AL.
†† Dynamic Test Engineer, NASA/Marshall Space Flight Center, Modal and Control Dynamics Team, Huntsville, AL.

motors are summarized in Table 1. Figure 2 presents a comparison between the RSRM and the potential five-segment full motor derivative configuration, which includes the forward skirt and frustum.

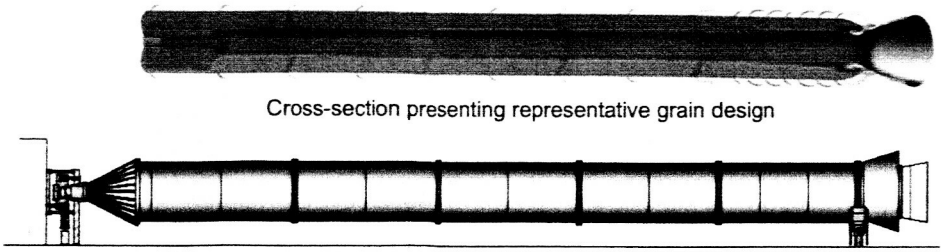

Figure 1 – ETM-3 Pictorial in T-97 Test Stand (at ATK Thiokol, Promontory, UT)

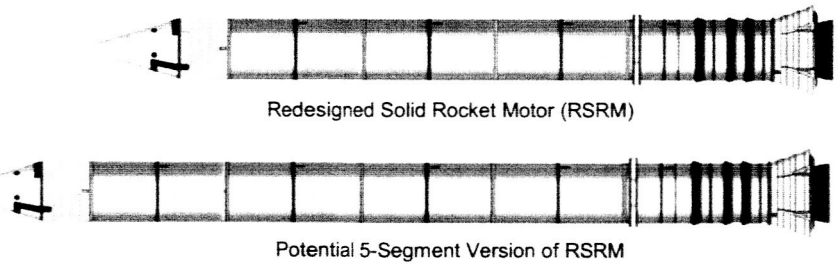

Figure 2 – Comparison of Current RSRM and Potential 5-Segment RSRM

Test Motivation

Although ETM-3 was designed as a margin test motor for the RSRM program due to its 5-segment configuration, this motor also assists in minimizing design risk of the Five Segment Booster (FSB) proposed for future launch vehicles. Both programs have and will continue to benefit from this 5-segment design, development, and static test fire. For example, a true margin test of critical parameters helps the RSRM program to better characterize its design uncertainties and their effects on Space Shuttle safety. Similarly, a FSB design benefits from a static fire by providing a beginning design database of performance and environment data for the new motor. The margin test, however, pushes the limits of not only the motor hardware but also the T-97 static test stand. As the T-97 test stand was designed to 4-segment induced loads, it became imperative that the math models of the system configuration of ETM-3 and the T-97 test stand be accurately characterized to insure a safe and successful static test firing. Accurate estimates of dynamic loads were required. Dynamic modal testing was implemented on ETM-3 to accomplish this test objective. In addition, possible coalescence of motor internal acoustic modes during static firing with the ETM-3 motor/stand vibration modes provided impetus for the modal test.[1]

T-97 Test Stand

A photograph and overview of the T-97 large motor static test facility with modal analysis equipment positions at ATK Thiokol in Utah is given in Figure 3; noted in the attached sketch are the modal survey equipment locations that were temporarily located to facilitate the subject modal test. The facility incorporates a removable building that covers and insulates the entire facility from external elements during assembly and preparation procedures. The subject modal test was performed with this structure in place (not shown). Sketches of the T-97 forward and aft stand support structures are provided in Figures 4 and 5, respectively. The complex nature of the test stand system requires detailed loads analyses to assure margin and safety factor requirements are met.

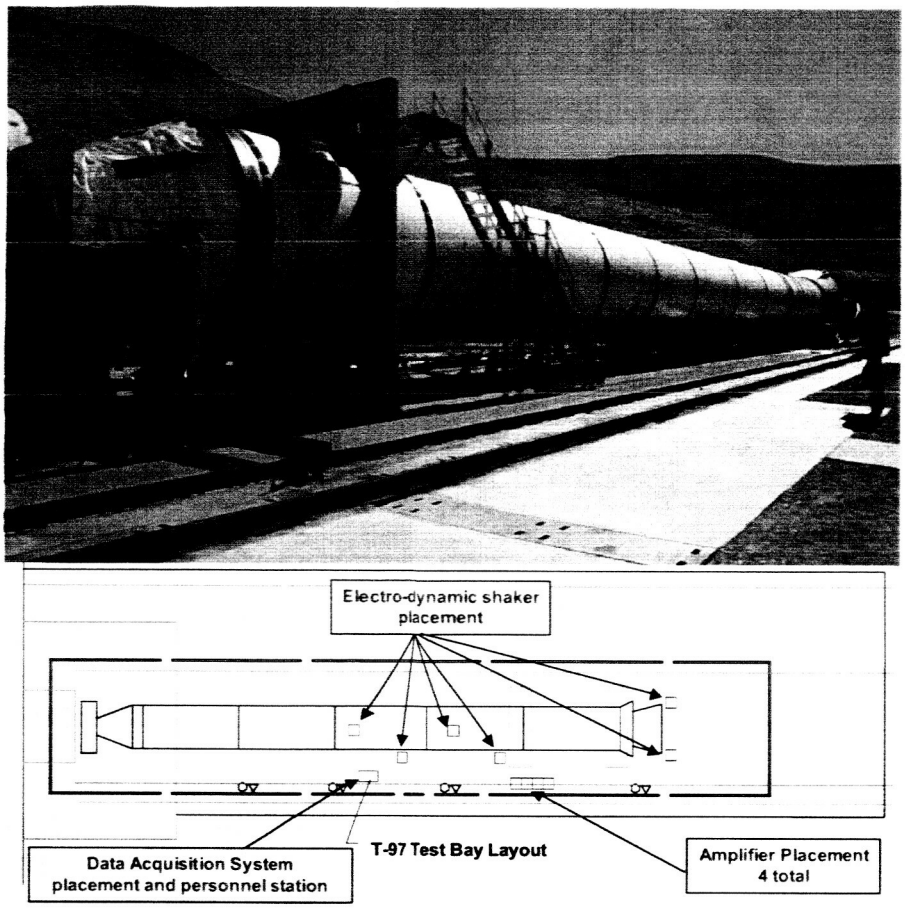

Figure 3 – ATK Thiokol T-97 Test Facility

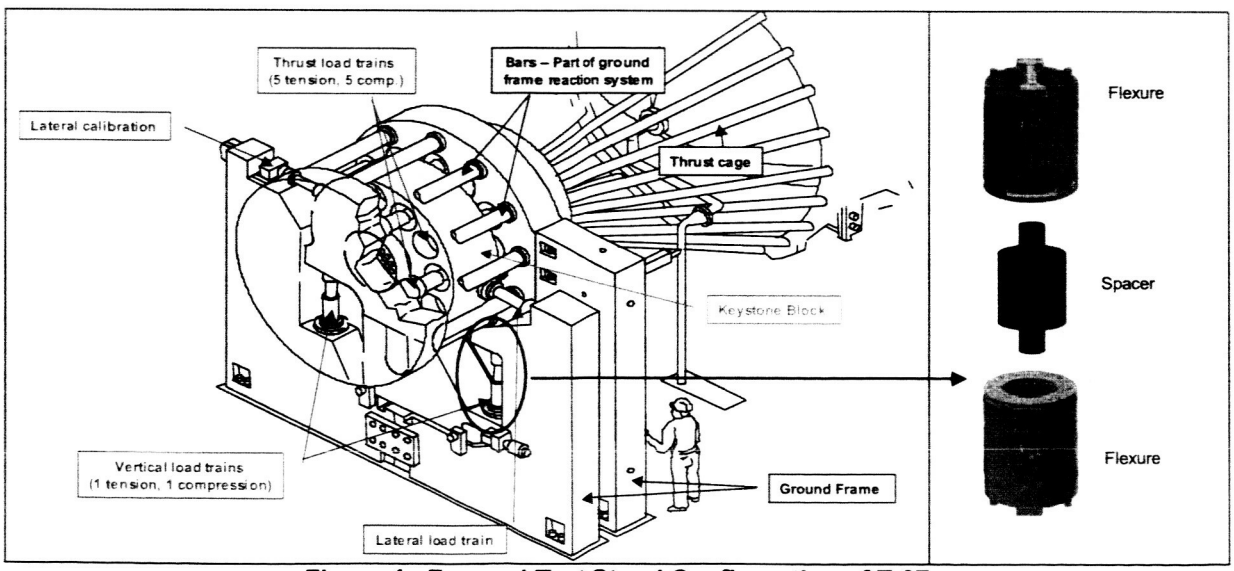

Figure 4 - Forward Test Stand Configuration of T-97

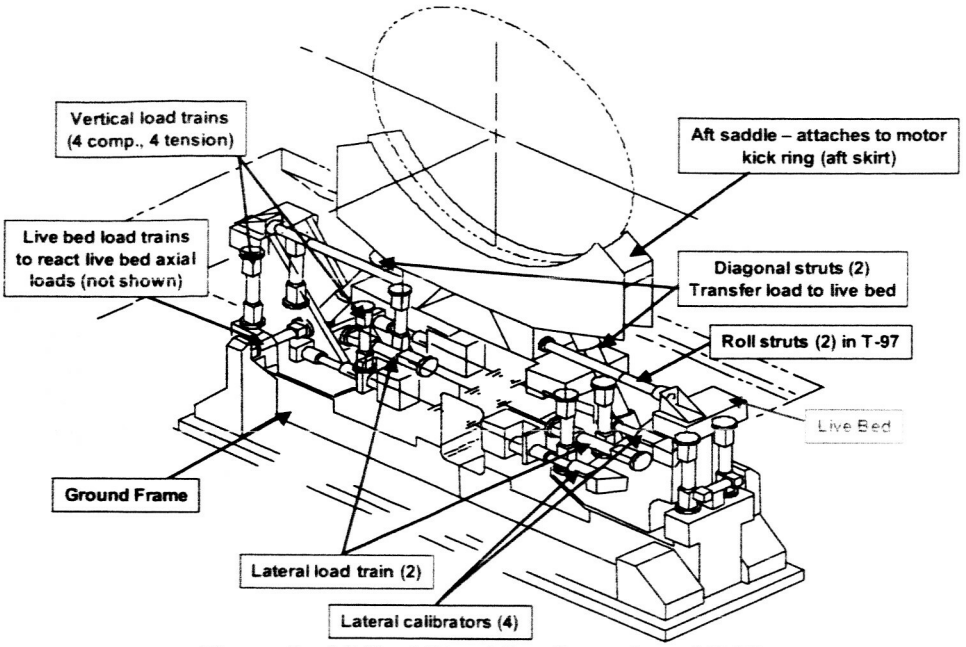

Figure 5 - Aft Test Stand Configuration of T-97

The forward stand consists of a large concrete reaction mass and multiple load train components. A longitudinal thrust calibration rod is employed to assure thrust measurement accuracy. Each load train component includes flexures that prevent transfer of moment loads and either load cells or instrumented struts. A large main pivot flexure is used to allow for the forward end motor rotation due to the effects of gravity loads. Axial, vertical, and lateral load trains are used to carefully monitor motor thrust characteristics during motor firing. The axial thrust loading is reacted through the main pivot flexure, a set of load cells, and into the concrete reaction mass (approximately 13.1 Mlb). The vertical loading is reacted through an instrumented tension and compression flexure system. Lateral loading at the forward stand is reacted through a single side load flexure and load cell system.

The aft test stand's primary purpose is to transfer vertical loading into the ground structure, stabilize the aft end of the motor and measure the motor burn thrust vector loads. The ETM-3 motor is bolted to the aft saddle, which transfers loading through two large diagonal struts into a structure call the live bed. The live bed is connected to the test stand ground through load train components similar to those of the forward stand. These include eight vertical flexures (four loaded in compression and four loaded in tension) two roll struts, and two lateral flexure and load cell systems. The aft stand also has eight large hydraulic anchors to connect the aft stand ground frame to the concrete foundation (not shown in Figure 5).

Previous Modal Survey Tests

In 1978, a full-scale model survey of the development motor, DM-3, was completed at the ATK Thiokol T-24 test stand facility in Utah. The purpose of this particular test was to identify the post-fire dynamic characteristics of the 4-segment Space Shuttle Solid Rocket Motor (SRM). Details of this test are found in Reference 2. This test was performed on a post-burn configuration; hence, the effects of a loaded motor were not measured. The post-burn study was motivated by a large thrust oscillation in the measured thrust data near end-of-burn. This concern is further discussed with respect to ETM-3. A second modal survey test was completed on Reclamation Motor #1 (RM-1) in 1988. This second modal survey test was also performed at the ATK Thiokol plant in Utah and involved a newly constructed test stand called T-97.[3] The RM-1 modal survey was a pre-fire test configuration in this newly constructed stand. Due to stress corrosion cracking in one of the forward stand flexures prior to testing, one of the major stand components was temporarily supported via alternate methods. Therefore, measured dynamic response was altered due to this configuration. The primary purpose of the RM-1 modal survey was to

provide the data necessary for dynamic math model correlation, and to prepare for implementation of a side load actuation system not previously used.

TEST ANALYSIS MODEL DEVELOPMENT

The RSRM finite element model previously generated in support of the 4-segment motor configuration was used to prepare a representation of the ETM-3 motor. This was accomplished by generating a second aft-center segment and joint section for inclusion in the Finite Element Model (FEM). The model consisted of a complete representation of the ETM-3 motor as well as the critical portions of the T-97 test facility. Figure 5 presents a pictorial of the ETM-3 FEM. As shown, the FEM provided representations of all major components of the motor along with detailed and previously validated representations of field joint interfaces. The main components included in the test stand (T-97) representation of the FEM included the major load train systems constructed of load cells, flexures and struts along with all connecting test stand structural elements to all locations considered to be grounded. Grounded locations included all points of contact with facility concrete structures in both the forward and aft test stand locations.

Previous detailed testing of flexure and load cell components, and previous modal survey and static test experience from the RSRM were used in establishing the ETM-3 FEM. Figure 6 provides a comparison of predicted finite element model modal frequencies for multiple burn time FEMs and static test measured data. These FEMs, representing various burn times (ignition and every 10 seconds after 50 seconds burn time) provided the analytical prediction capability to develop design loads for structural analysis.

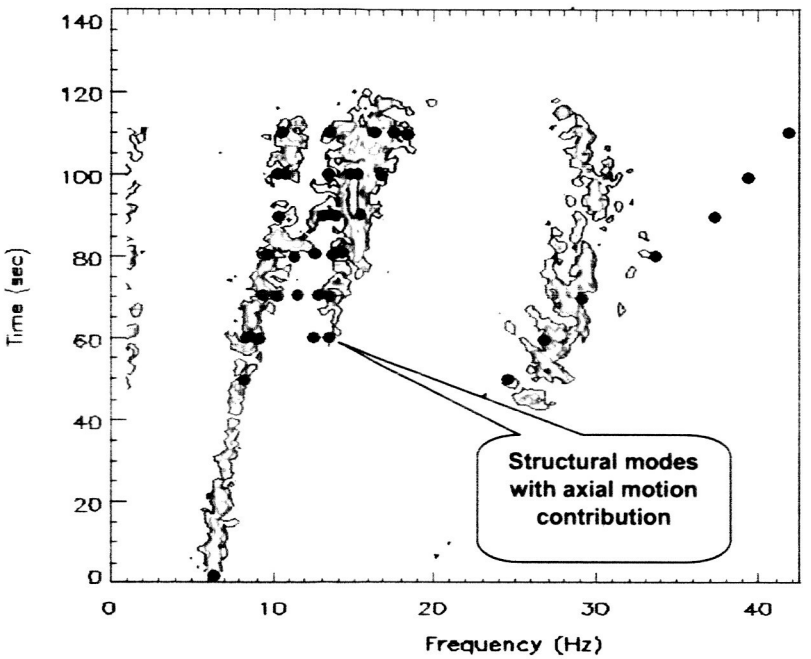

Figure 6 – Comparison of RSRM FEM Predicted Axial Modes to Measured Load Train Data

The detailed FEMs (Figure 7) consisted of a significantly higher level of fidelity (300,000+ DOF) than could be represented in a modal test setup. Therefore, a reduction of the total degrees-of-freedom was desired to develop the TAM. Mode expansion was considered, but not pursued due to the desire to have on-site test-to-analysis comparison capabilities. Prior to selection of the appropriate analysis set Degrees-of-Freedom (DOF), pre-test analyses were performed, and the target modes were selected.

As test stand components would be loaded during the modal survey, pre-test analyses were performed to determine resultant loads from random and sinusoidal load excitation via the electrodynamic shakers. These analyses studied the total forces and displacements that would be expected during testing. Figure

8 provides a pictorial of one such analysis reviewing the resultant forces in various test stand components. This analysis considered input sinusoidal loading of 300 lbf.

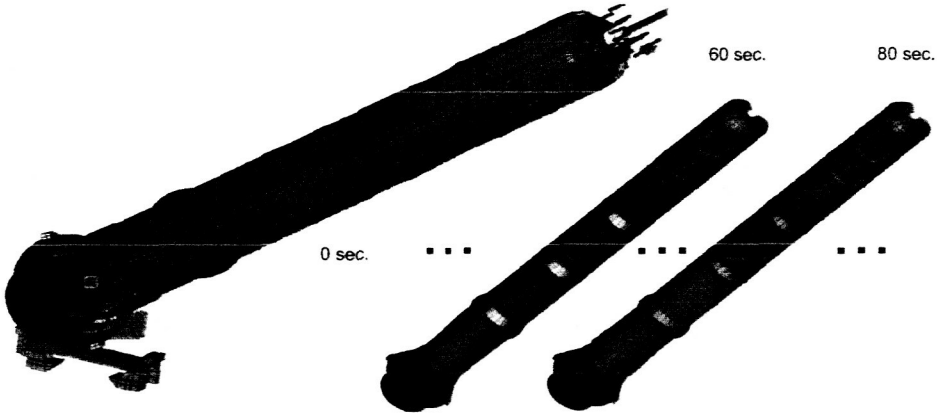

Figure 7 - ETM-3 Finite Element Models with T-97 Components

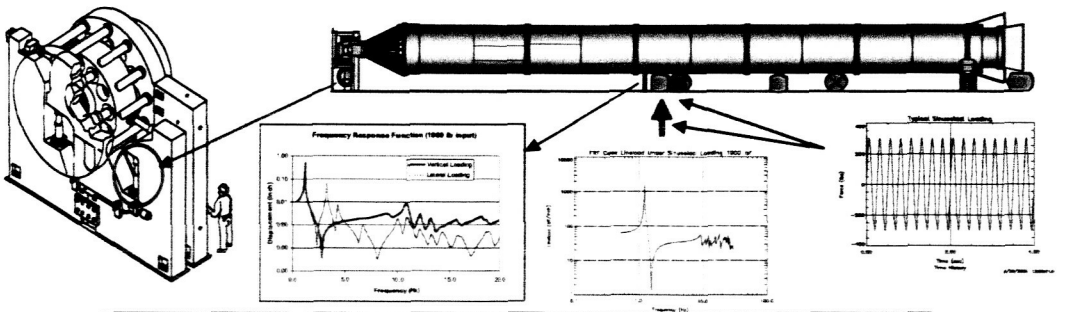

Load Train	Max Force (lbf)	Design Load (lbf)	Gravity Loads (lbf)	Delta (lbf)
Forward Vertical	22300	401100	392700	13900
Forward Lateral	37400	40000	0	-2600
Aft Diagonal	47200	851200	506100	-297900
Aft Vertical	12200	220100	117300	-90600
Aft Lateral	19800	176100	4900	-151400
Motor center deflection 0.2 inch reaches design load on forward vertical tension load train				

Figure 8 – Finite Element Analysis of Modal Survey Loading Effects on Subject Structure

The results indicated that care must be taken during sinusoidal testing to assure that induced loads on the forward vertical tension flexures remain below design loads; this concern was related to flexure thread yielding and re-use issues; although margin existed with design loads, it was determined unacceptable to load these flexures beyond design limits as a result of this testing.

As Multiple Input Multiple Output (MIMO) burst random testing was planned, several additional analyses considering MIMO conditions were reviewed. The studies resulted in establishment of limit response conditions to be monitored via LVDT and strain measurements. An electronic power cut-off system was implemented to automatically power-down the shaker amplifiers should these conditions be exceeded.

The final pretest analyses consisted of prediction of the gravitational load effects on the assembled motor in the test stand. The finite element model was used to determine total distance from the concrete floor to the motor case for design of the electrodynamic shaker stands as these stand had to be fabricated well before the motor was assembled and prepared for testing. The stands had to be sufficiently rigid so as to prevent excessive shaker motion during testing in the frequency range of interest. Modal analyses were used to evaluate the stand design with the shakers attached. These pre-modal test preparation studies

proved very valuable as no modifications to the stands were required and the shaker support system functioned very well even with the large mass of the chosen shakers. Noted was that the original support stand design was proven insufficient via these analyses, and the deficiencies were corrected prior to any significant impact. Figure 9 presents a comparison of the predicted results with actual measured conditions and presents an example of the test stand modal analyses. Measured data indicated by "Shaker Attach Locations" and the displacement gage labeled, "DVQCI001".

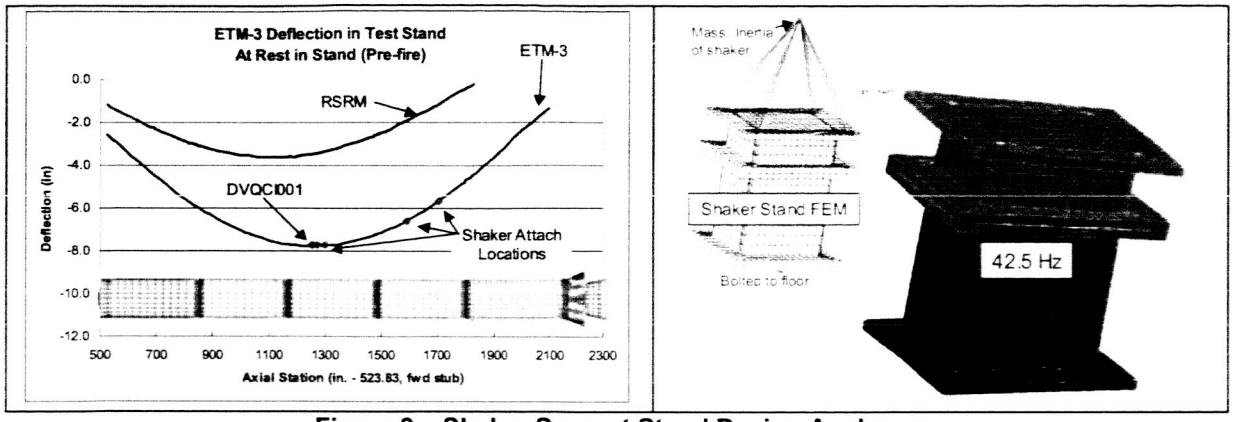

Figure 9 – Shaker Support Stand Design Analyses

Selection of Target Modes and Pre-test Analysis

The T-97 facility was constructed originally to accommodate a 4-segment RSRM, and was designed to support the loads produced by a 4-segment RSRM. The increased forces resulting from the ETM-3 motor firing and added mass challenged the forward test stand design margins. Table 1 provides a relative comparison of RSRM vs. ETM-3 mass, length and thrust.

Table 1 – Relative Comparison of RSRM vs. ETM-3 Design Parameters

Parameter	RSRM	ETM-3
Unsupported Length*	1.00	1.24
Motor Mass*	1.00	1.26
Motor Thrust*	1.00	1.09
Configuration	4 segments, Standard nozzle	5 segments, Extended Nozzle
* Data are normalized to RSRM parameters		

Concerns for potential dynamic response conditions resulting from coupling of internal motor acoustics and combined system (motor and test stand) structural modes required significant study. As a result, a prediction method for internal motor acoustic response due to flow vortex excitation and random combustion, and the resulting thrust effects was developed and is the subject of separate paper.[1]

Additional analyses of previous RSRM measured loads and acceleration data were performed to review frequency content and response magnitudes associated with static test generated loads and environments. Figure 10 provides a contour plot of a typical measured load cell response from a previous RSRM motor firing. As shown, the RSRM demonstrated coupling of the internal chamber acoustic mode with a significant structural mode in the test configuration during latter burn times.

As the ETM-3 motor designed performance well exceeded that of the 4-segment RSRM, and potential for coupling of these two modes during higher loading conditions existed, the concern for better understanding the ETM-3 structural modes and model validation would be satisfied by the subject modal survey. Further discussion on the acoustic-structural mode coupling, and details of prediction study results for both the RSRM and ETM-3 are provided in the previously cited paper.[1]

The ETM-3 motor case/joint components and T-97 test stand load cell and flexure components were of most concern. Generated loads affecting these components are due to superposition of the lower-order structural mode responses. The lower frequency (less than 20 Hz) structural modes were of interest with

further concentration on modes with potential to influence forward stand axial, lateral and vertical load train forces as well as aft stand lateral forces. Modes with potential to cause additional field joint loading were also of concern.

The FEM was used to compute the mass participation factors for each mode and to review the modal strain energy contributions to specific components of interest. Figure 11 presents the cumulative modal effective mass fraction for modes up to 20 Hz. As shown, the significant majority of modal mass is included in these modes. A readily available Commercial-off-the-Shelf (COTS) finite element solver facilitated both of these selection methods. Table 2 presents a description of these modes, which included lower order bending modes, axial and roll modes, and additional motor shell and test stand related modes.

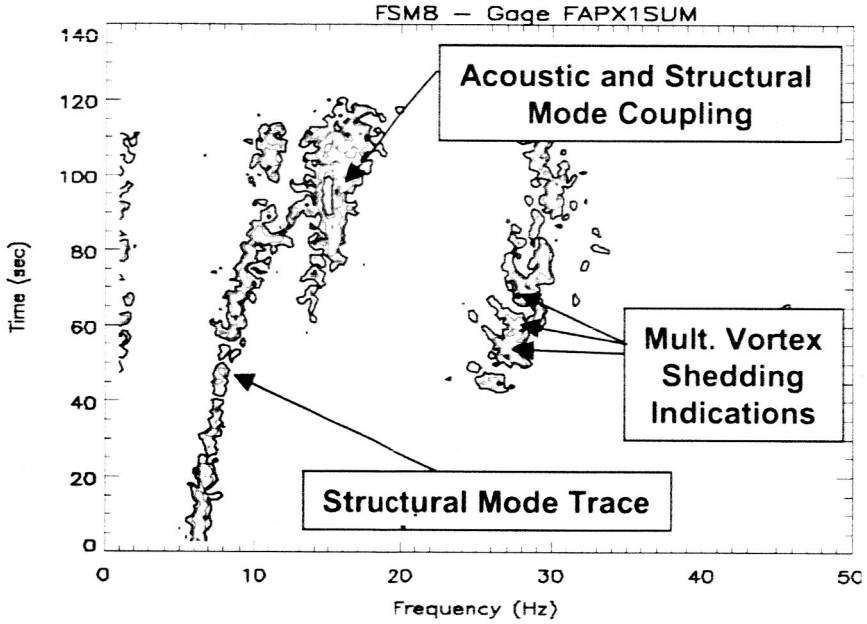

Figure 10 – Example RSRM Static Test Load Cell Spectrum

Expected modal damping varied from 0.5% to 4%. The lower values were associated with bending and roll modes, and the higher damping was expected with the axial and nozzle vectoring modes. It was the intent of the modal surveys to detail additional modes up to 20 Hz for objectives other than design loads development validation.

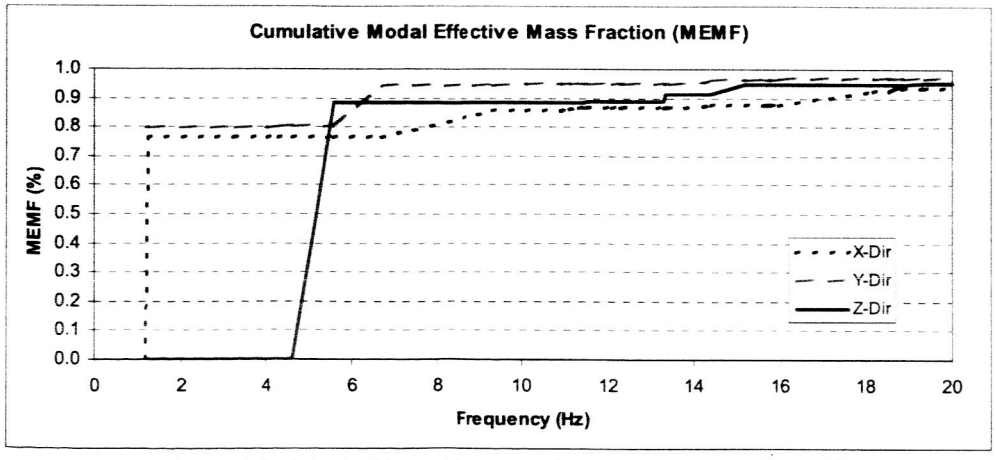

Figure 11 - Modal Mass Fraction from ETM-3 in T-97 FEM

Table 2 – ETM-3 Modal Survey Target Modes and Predictions

Mode Description	ETM-3 Ignition (Hz)	ETM-3 End-of-Burn (Hz)	Modal Effective Mass Fraction
First Lateral Bending	1.2	3.7	76 – 79% Translation
First Vertical Bending	1.3	3.9	59 – 64% Rotation
First Roll	3.3	7.3	44% Rotation
Second Lateral Bending	4.3	13.8	25% Rotation
Second Vertical Bending	4.6	14.0	8% Rotation
First Axial	5.6	15.3	88% Translation
Lateral Bending/Stand Lat.	6.7	9.1	14% Translation
Third Vertical Bending	9.3	n/a	9% Translation
First Shell	10.9	5.1	<1%

Analysis Set and Excitation Selection

Once the target modes were selected, the analysis set locations required identification. Previous experience with solid rocket motor TAM development has indicated that a standard approach using static reduction would yield a poor TAM due to the high mass to stiffness ratio conditions associated with this type of structure.[4] As a result, a hybrid method known as the Effective Independence Method was employed via a specially developed finite element solution alteration to arrive at a candidate analysis set.[5,6]

In order to provide the potential to measure lower order motor shell modes and provide opportunity to further understand propellant dynamic modulus, it was determined that a set of approximately 200 analysis set DOF would be used. This would allow additional channels of a 256 channel Data Acquisition System (DAS) for strain, loadcell and displacement data acquisition. Additional detail on the analysis set selection process is provided below. The excitation locations were selected based on energy methods and engineering judgment.

Effective Independence

The objective of the Effective Independence Method is to select analysis set DOF (or locations) to maximize the linear independence of the target mode shape partitions. At the same time, the method seeks to retain as much information about the target modal responses as possible. Target test mode independence provides required data for analysis to test data correlation. The method relies on the accuracy of the finite element model to the extent that the general eigenvector resembles the actual mode shape enough to effectively select these degrees-of-freedom. The method employs an iterative solution starting with a candidate DOF set, proceeds to rank each DOF's contribution to the eigenvalues of the TAM, and then drops the DOF exhibiting the lowest contribution; the algorithm continues to iterate until the desired number of analysis set DOF's have been located. An extension of the method is to select the candidate set by enforcing that all three translation degrees-of-freedom must be selected as a set thus producing a set of N 3-DOF locations resulting in a total of 3N analysis set DOF. This method allows for a more visually recognizable TAM that can be used during the test. The details of the Effective Independence Method are not discussed herein. However, Kammer provides further details.[5] Several analyses with various desired analysis set DOF were performed. The final selection was based on a set of 75 analysis set DOF thus allowing for additional DOF to be selected by engineering judgment.

Engineering judgment was used to augment the results, and cross-orthogonality results were used to validate the effectiveness of the candidate set. Figure 12 presents a pictorial of the original ignition configuration FEM and the final TAM using the Effective Independence results combined with additional DOF selected by engineering judgment. The Effective Independence Method was found to return selected DOF that achieved very good cross-orthogonality values for the target modes. However, the DOF distribution made visual recognition somewhat difficult and as such was considered insufficient for on-site test TAM comparisons. Noted is the argument that the majority of the modes could have been captured simply by engineering judgment due to the simple beam characteristics inherent in the problem. However, where the method provided significant contribution in selecting an effective analysis set was with conditions where significant modal contribution was exhibited by materials with low stiffness and a large contribution to the modal mass (high M/K conditions). Analysis set locations could only be chosen

on the external surface of the motor and stand components. Previous testing performed in a single RSRM segment clearly identified the improvements obtained with respect to this issue, and higher order modes, although not selected as target modes with respect to design loads verification, were desired to assist in separate objectives.[4]

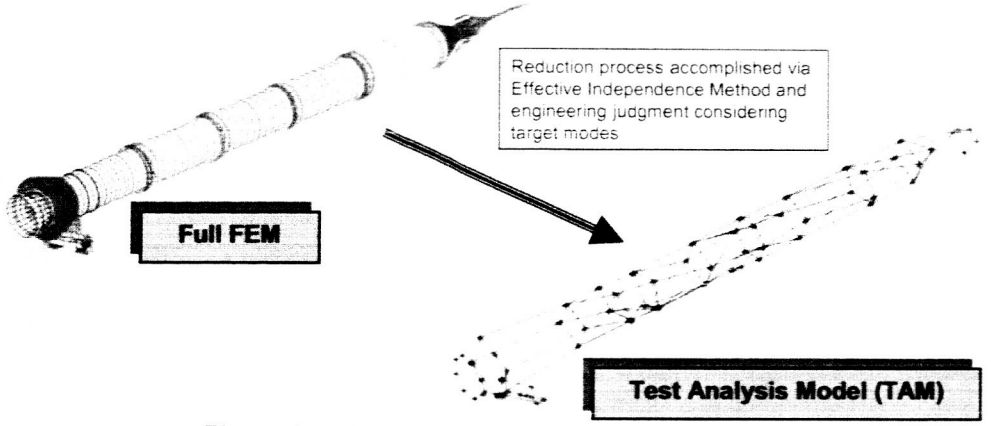

Figure 12 – Comparison of Full FEM to TAM DOF

Parameter Sensitivity Study

As the ETM-3 FEM was an extrapolation of the previously correlated RSRM FEM, it was expected that the ETM-3 model would be a reasonably accurate representation of ETM-3, and would therefore be capable of generating reasonably accurate component loads (assuming the input motor performance parameters were also reasonably accurate). However, in order to consider a range of errors in modal parameters and subsequent effects on resultant loads, a sensitivity study was performed to determine model parameters of most interest. The desired result from this study was to reveal that the largest sensitivities would be related to variables that were well defined. Figure 13 provides a detailed bar graph presenting normalized modal frequency sensitivities for the selected parameters. The parameters exhibiting the highest influence on the FEM modal frequencies were found to be well understood and characterized. The results of this study enhanced confidence that the generated FEM was accurately predicting motor and test stand structural response.

One item of interest was that the critical axial mode of the motor in the test stand was significantly more sensitive to the motor case modulus than to the flexures and load cells in the forward test stand. Previous modal strain energy analyses had also indicated similar findings, but the sensitivity analyses detailed this very clearly. This further increased confidence in prediction of this axial mode, and the relationship of this mode to the internal motor acoustic response.

The information provided by the sensitivity study suggested modifications to parameters for the purpose of performing a pre-test parametric study of the effect of modal frequency shifts in resulting transient loads. These analyses considered a variation of ±20% on modal frequency shifts as well as modal damping. Figure 14 provides the target modes with the highest effective mass fractions and the evaluated frequency variations in the loads analyses. A detailed discussion of these analyses is not included herein. However, it is noted that the study further increased confidence in generated design loads for ETM-3. Post-test results are also included in Figure 13 for comparison; as shown, the modal survey frequencies fell well within the examined conditions with the exception of the third lateral bending mode. This mode however, exhibited significantly lower effective mass and small strain energy influence on structural components of concern.

These studies added confidence to both the accuracy of the ETM-3 FEM prior to performing the modal survey, as well as the design loads generation work performed to support design and analysis efforts.

In order to validate the assumed conditions, the modal survey test results were required. Although previous modal survey history had provided a valuable basis for assumptions on modal damping, a modal

survey of ETM-3 was the sole method of obtaining this parameter for the critical modes. As discussed below, this proved very valuable in review of the extracted modal parameters.

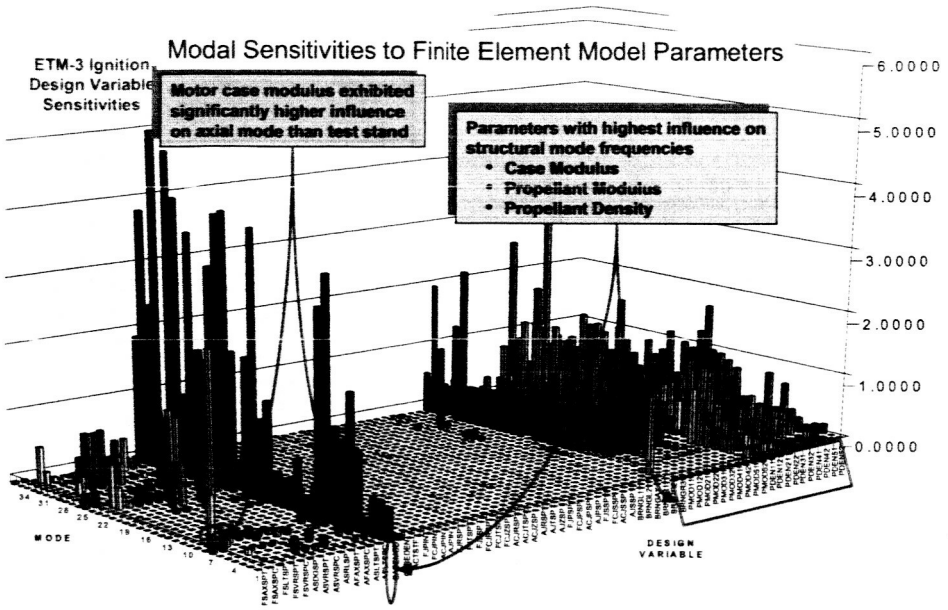

Figure 13 – ETM-3 in T-97 Sensitivity Study

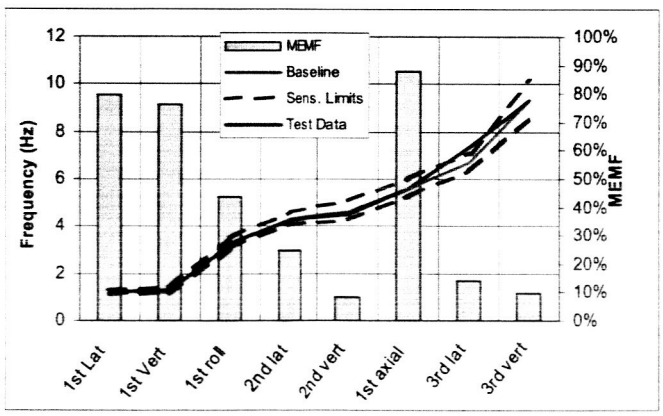

Figure 14 - Load Sensitivity Study Frequency Shift Considerations for Significant Modes

As a final comment on the analysis activities, it is noted that in most applications there remains little time between completion of a modal survey on a large space structure and the scheduled use of that structure. These sensitivity and parametric studies were performed in order to provide tools for rapid analysis response for approval to fire the newly designed 5-segment motor.

TESTING PROGRAM

Two separate modal tests were conducted on the ETM-3 motor by the NASA Marshall Space Flight Center (MSFC) Modal and Control Dynamics Team. The pre-fire motor test was conducted in September 2003 just prior to the planned motor firing, and the post-fire motor test was conducted in November 2003. The following paragraphs primarily discuss the testing program for the pre-fire motor although test conduct for the post-fire modal test was very similar.

For the pre-fire motor modal test, analysis identified 84 measurement locations on the motor and the two test stands. Two types of accelerometers were used to measure the modes in a 0-32 Hz bandwidth. Since the pretest finite element model predicted the first bending modes at just above 1 Hz, several high sensitivity DC capacitive accelerometers were strategically placed along the motor to facilitate measurement of these modes. A total of 14 triaxial DC accelerometers (PCB Model 3701M15) were used along the length of the motor. An additional six uniaxial DC accelerometers at each of six excitation locations to produce higher fidelity data in the lower frequencies as well. The remaining measurement locations were instrumented with standard ICP modal accelerometers (PCB 333).

Excitation was provided using a total of six Unholtz Dickie Model 6 electrodynamic shakers, two in each axis. Only two shakers were operated simultaneously, providing excitation to one of the three orthogonal axes at a time. Two of the shakers were attached to the hold down posts at the aft end of the motor. The two lateral shakers were located near the center of the motor and between the center and the aft end of the motor. Likewise two vertical shakers were installed near the center and the aft/center of the motor. Each shaker was attached through a metal pad, which was bonded to the motor case using dental cement (Tridox F88); this was a unique approach devised to allow attachment to the cylindrical motor case structure in an unobtrusive and non-destructible manner. For the two lateral shakers, the attach pad was included an angle bracket to facilitate both lateral and torsional excitation. PCB 223M12 load cells were used to measure the input force. A typical shaker setup is shown in Figure 15. The support equipment for the electrodynamic shakers were custom fabricated to accommodate the motor deflection conditions due to gravity loads on the structure.

Frequency response functions (FRF's) between the output responses and the input forces were acquired using a Leuven Measurement Systems (LMS) Scadas III data acquisition system controlled by LMS CADA-X software. A total of 256 channels were acquired simultaneously. The accelerometers accounted for 240 channels and the load cells accounted for two channels per run. The additional 14 channels were various force, strain, and displacement instrumentation, which were part of the ATK/Thiokol test stand. The NASA/MSFC test equipment is shown in Figure 16.

During the pre-fire motor modal survey, two conditions were tested. These two conditions involved different forward test stand preload conditions that are produced via the test stand calibration system. As the motor burn conditions include a thrust load greater than 3 Mlbf it was desired to obtain modal parameters in a loaded stand configuration. It was also desired to investigate any non-linearities from an unloaded condition to the loaded condition. The first test condition had no preload applied to the test stand. Standard Multi-Input Multi-Output (MIMO) techniques were used to acquire the test data using two shakers at a time. The input excitation was burst random with a force level of approximately 120-140 lb_{rms}. For each excitation axis, five minutes of time history data for the random excitation was also acquired as supplemental data. After MIMO data were acquired using all six shakers, a 1 Mlbf axial preload was applied to the test stand. Although the 1 Mlbf load was well below expected motor thrust conditions, this load was sufficient to evaluate any non-linearities. All testing was repeated for the preloaded configuration.

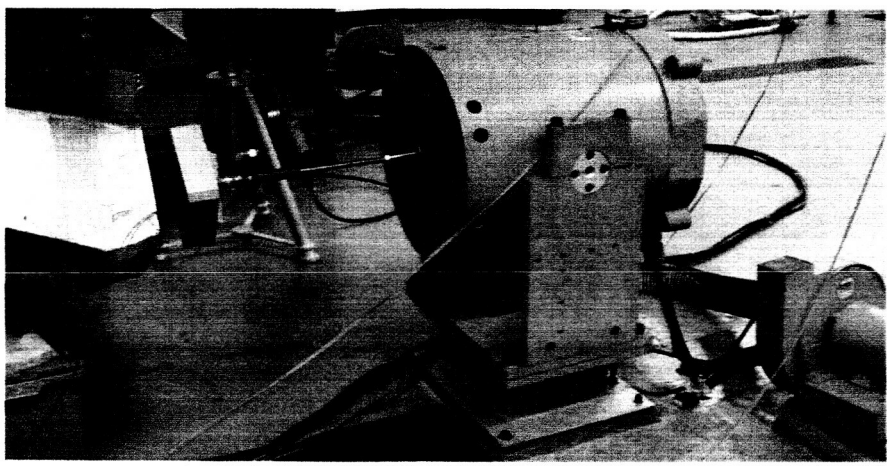

Figure 15 – Typical Shaker Setup

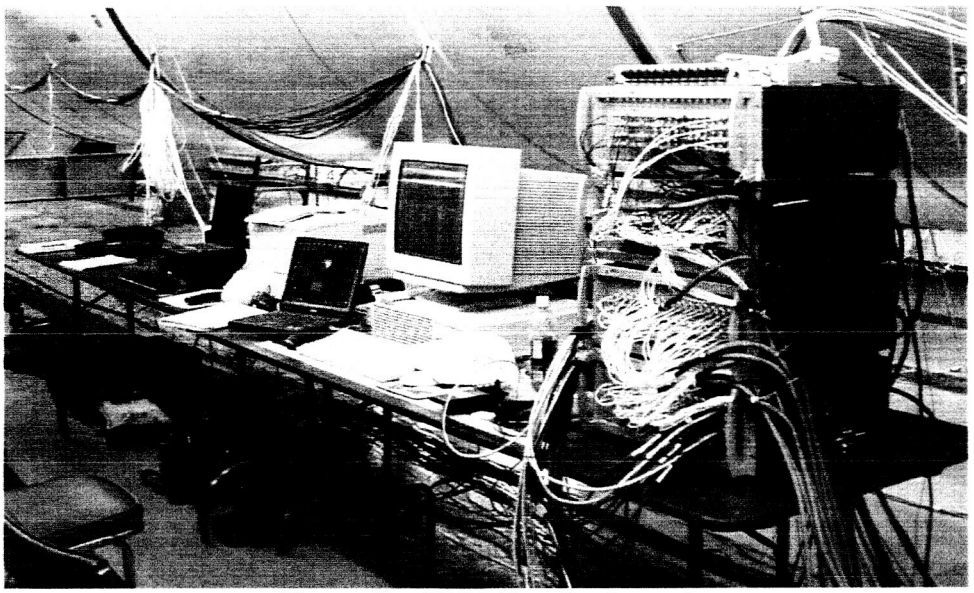

Figure 16 – MSFC Test Equipment

Sine sweeps were also used for the preloaded stand conditions to further identify and characterize any force-dependent non-linearities. Narrow band sine sweeps in each axis using one shaker at a time were used to acquire drive point FRF's at varying force levels. A Hewlett Packard 3562 two-channel dynamic signal analyzer was used for this phase of the testing. The maximum sinusoidal load of 300 pounds force was required in the axial direction. For sine sweeps in the lateral and vertical direction, a maximum of 100 pounds was used. The maximum measured structural displacement at the center of the motor was approximately 0.2 in. peak-to-peak at resonance during the highest force level sweep in the vertical axis.

At the conclusion of the planned testing, an additional series of tests was added to continue the study of the critical axial mode. A comparison of the no-preload configuration and the preloaded configuration revealed that the axial mode shifted approximately 7% from 5.2 Hz to 5.6 Hz. Other modes were not affected. Concern for a continued shift in frequency with increased loads prompted additional testing at higher test stand preload levels. Four additional burst random tests were conducted at four different stand preloads – no preload, 1 Mlbf, 1.5 Mlbf, and 2 Mlbf. Only 15 averages were acquired for each of these tests to minimize the time during which the test stand was preloaded at the maximum of 2 Mlbf. Figure 17 shows the axial drive point FRF's for this incremental preload testing. The results revealed that the axial mode frequency did not continue to increase with additional increases in the motor preload and indicated that the observed non-linearity was associated with an inherent decrease in stiffness of the test stand axial load train components when unloaded. This was not originally expected, as previous testing indicated no differences but this condition posed no concerns.

Modal parameter estimation using LMS CADA-X software identified 23 modes for each of the test configurations in the pre-fire motor modal survey.

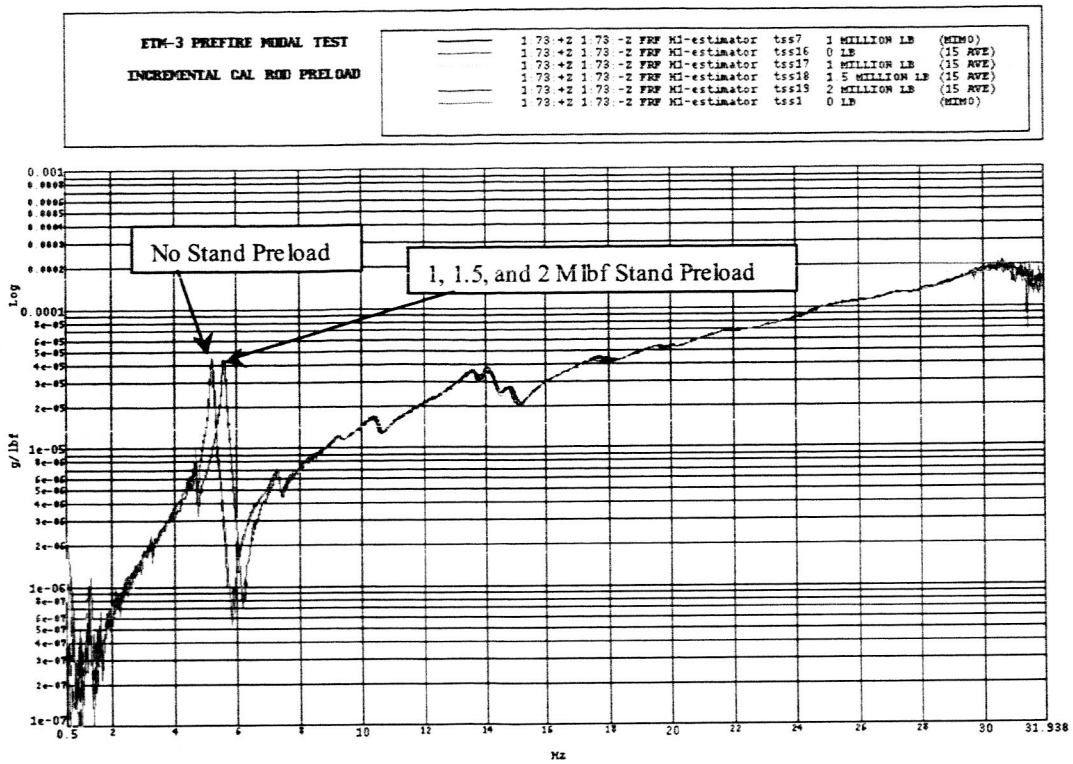

Figure 17 – Axial Drive Point FRF During Incremental Preloading

MODAL SURVEY RESULTS

The test results for the target modes are provided in Table 3. The remaining test results are documented in References 7 and 8. Also included in Table 3 are the pre-test FEM results for comparison purposes. The observed damping for the critical first axial mode was half that originally assumed from previous studies. This was the most revealing finding from the test as the remaining modal frequencies represented a close match to the pre-test predictions, and the remaining damping parameters were either higher than assumed or associated with modes exhibiting smaller modal effective mass.

Table 3 – Comparison of Modal Frequency and Damping Values for Test and TAM

Target Modes (Load Producing Modes)							
	Pre-Test Analysis		Test Results		Comparison		MEMF
Mode Description	FEM Freq. (Hz)	Damping (Verification)	Test Freq. (Hz)	Damping	Freq. Diff. %	Damp. Diff. %	% of Total
1st Lateral Bending	1.19	0.5%	1.22	1.1%	-2.1%	120.0%	79%
1st Vertical Bending	1.25	0.5%	1.29	0.8%	-3.1%	60.0%	76%
1st Roll	3.28	0.7%	3.26	0.7%	0.7%	0.0%	44%
2nd Lateral Bending/Nozzle Torsion	4.29	0.7%	4.51	0.7%	-5.0%	0.0%	25%
2nd Vertical Bending	4.63	0.7%	4.72	0.4%	-1.8%	-42.9%	8%
1st Axial	**5.59**	**2.0%**	**5.60**	**1.0%**	**-0.2%**	**-50.0%**	**88%**
3rd Lateral Bending	6.70	1.0%	7.36	0.9%	-9.0%	-10.0%	14%
3rd Vertical Bending	9.33	1.0%	9.35	0.9%	-0.2%	-10.0%	9%
First Shell	10.94	2.0%	13.30	2.2%	21.6%	10.0%	<1%

Figure 18 presents mode shape plots for the high modal effective mass modes. The test obtained modal frequencies are repeated from Table 3 in parenthesis.

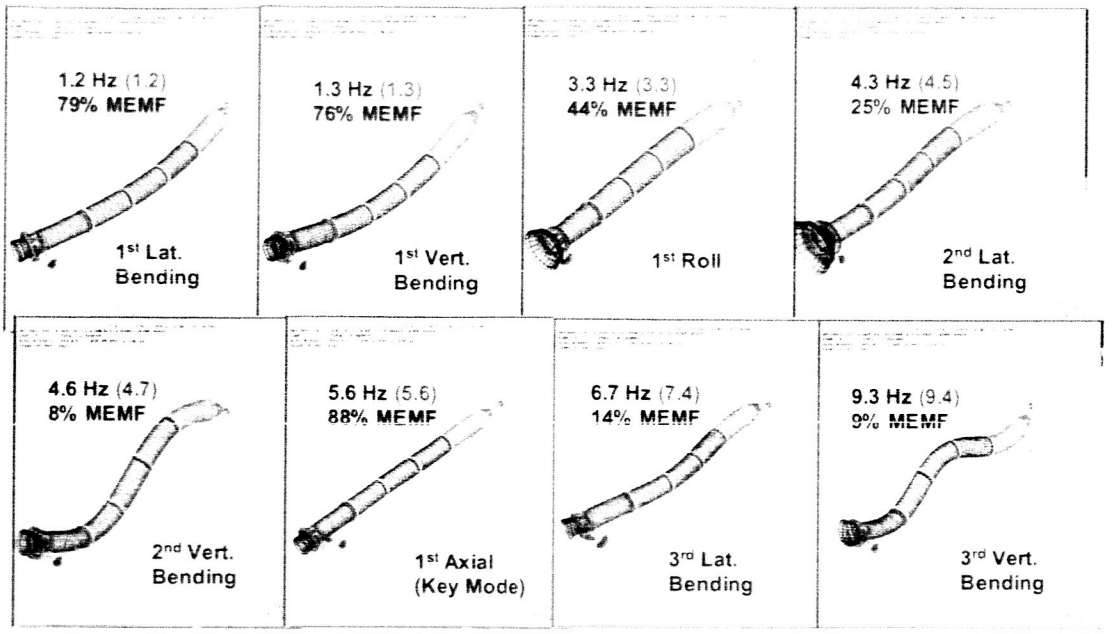

Figure 18 – Pictorials of ETM-3 Mode Shapes for High Modal Effective Mass Modes

Figure 19 provides a review of the cross-orthogonality data between the test and analysis modes for the critical (or target) modes with high modal effective mass. Also included are two additional modes not considered target modes that fall in the observed test and analysis mode order. As shown, an excellent correlation was observed. The off-diagonal terms were less than 0.2 in almost all cases indicating good test to analysis mode independence.

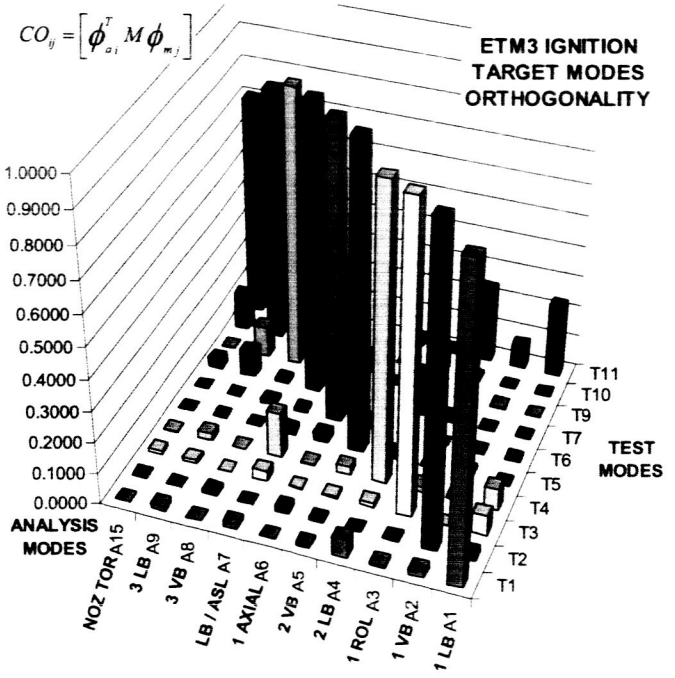

Figure 19 – Cross-Orthogonality Comparison between Test and TAM Modes

CONCLUSIONS/FUTURE WORK

Justification for ETM-3 Test Fire

As presented in the sensitivity study section, pre-test analyses examined the effect of modal frequency variability in relation to other motor boundary loads and internal motor acoustic response. A comparison of the resulting modal frequencies and damping with the pre-test predictions rapidly provided rationale for approval to fire ETM-3. Based on the pre-test sensitivity studies and parametric loads analyses, the observed lower first axial mode damping was the only concerning discrepancy between the pre-test FEM assumptions and the test-measured data. The difference was outside the pre-test loads sensitivity study limits and was associated with a critical, high MEMF mode. In order to review the impact of this condition, delta-loads analyses assuming the modal test obtained damping parameters for all target modes were performed. Analyses for ignition and sustained burn conditions were reviewed accounting for potential coupling of the internal motor acoustic response with this axial mode. Figure 20 presents one set of results for these analyses and was associated with combined worst-case performance conditions. This example considered worst-case excitation of the second axial acoustic mode (2-L) coupled with the modal survey observed first axial motor mode adjusted for motor burn time. Potential resonance condition loads remained below design loads. Again, it was not the intent of this paper to detail the loads analyses. However, it is sufficient to note that the modal survey results provided valuable data to facilitate a quick-look assessment of modal parameter differences between FEM predicted (or assumed) and test data; these data were used to verify design loads development tools and in turn, further justify the design loads themselves. The results provided rationale to proceed with firing ETM-3.

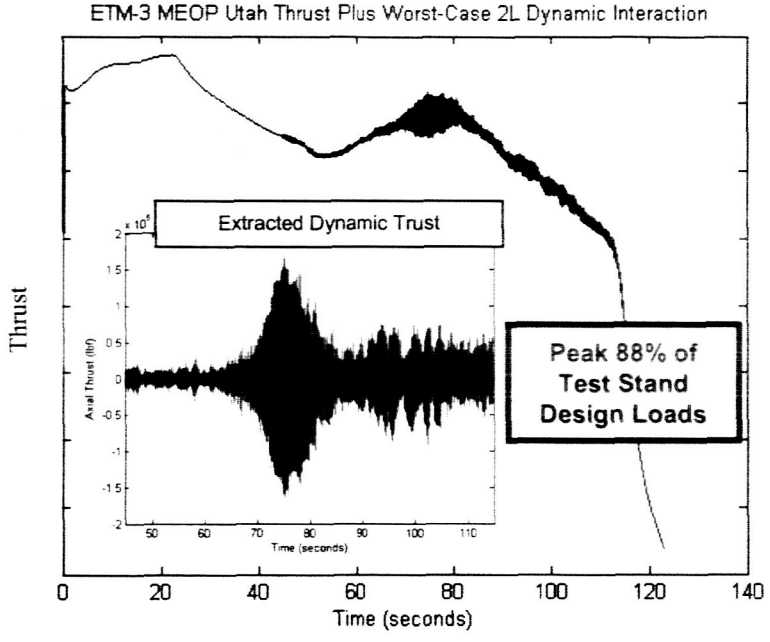

Figure 20 – Example Results from Transient Analyses Justifying ETM-3 Firing

Post-Fire Comparison Comments and Lessons Learned

Post-test data were analyzed and used to track modal response during motor burn. Figure 21 provides an example of such data. The results indicated modal response as expected. Figure 22 provides a comparison of the pre and post-test modal survey data with the obtained acceleration response data from the firing of ETM-3. As shown, the modal test results were observed clearly in the motor firing data. The acceleration data from the ETM-3 firing provided valuable data to track changes in the modal frequencies, and the post-test modal data provided a reference to each modes end-of-burn characteristics. The post-

fire survey is not detailed herein, but these results are presented to convey the overall behavior to the reader.

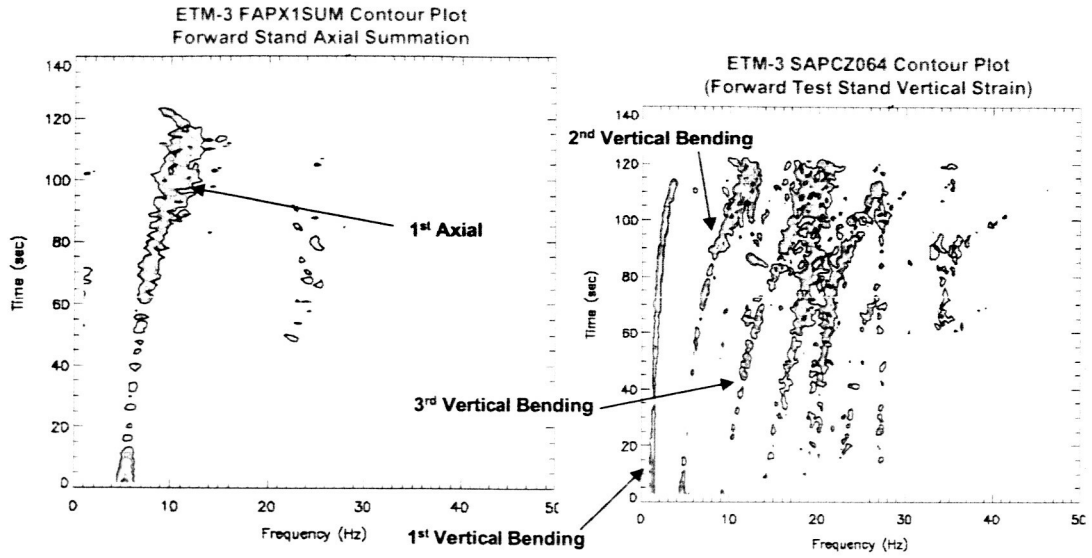

Figure 21 – Example of ETM-3 Firing Measured Mode Traces

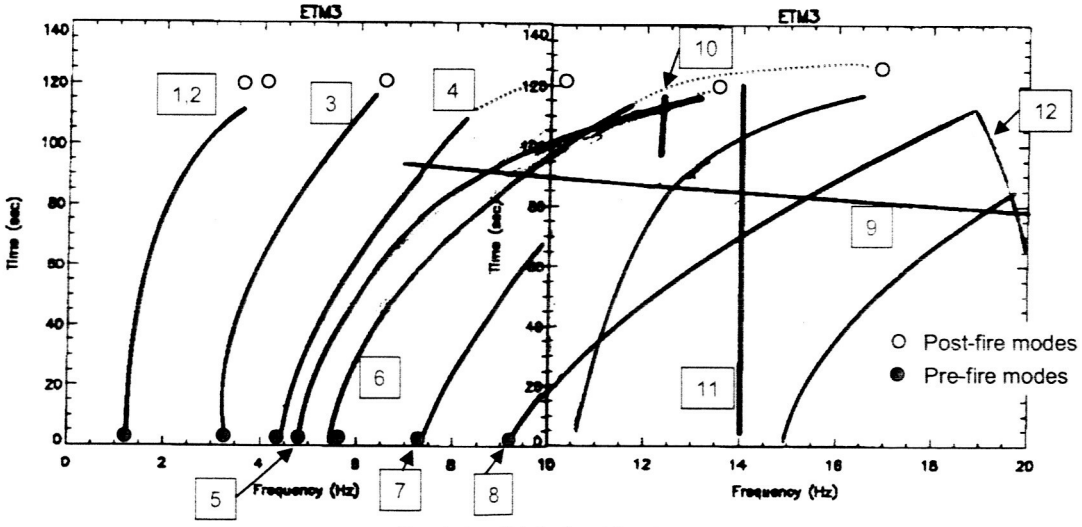

Description of Modes from Motor Burn Data

(1) 1st lateral bending	(5) 2nd vertical bending	(9) TVC activity
(2) 1st vertical bending	(6) 1st axial	(10) 1-L acoustic mode
(3) 1st roll	(7) 3rd lateral bending	(11) Live bend axial
(4) 2nd lateral bending	(8) 3rd vertical bending	(12) Nozzle n = 2 shell

Figure 22 – Test Data Derived Composite Modal Frequency Traces for ETM-3

As the motor burns, it becomes more difficult to extract modal frequency information from the acceleration data. However, the data provided confidence that the developed FEMs for the additional burn times also provided a very good representation of the actual conditions.

Figure 23 presents a pictorial of measured motor thrust oscillations that is directly comparable to the pre-test worst-case 2-L prediction presented in Figure 16. Note that the dynamic content is significantly less

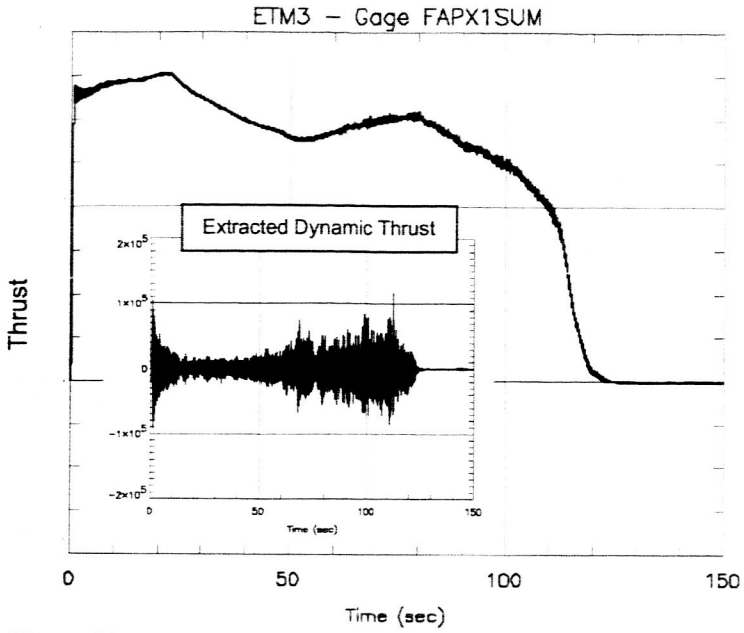

Figure 23 – Measured ETM-3 Thrust and Extracted Dynamic Thrust

than predicted for worst-case conditions. It is noted that the ETM-3 dynamic thrust was actually less than historical RSRM behavior. Recent studies (as well as the ETM-3 test data, although one motor firing does not provide justification for any statistical assessment) indicate that changes made in the 5-segment configuration design of ETM-3 may result in lower than expected excitation of internal acoustic modes and thus reduced potential for thrust oscillations relative to RSRM history. Additional study and motor performance data is required to fully justify this inference.

Although readily available commercial software provides excellent tools for performing complex modal and transient analyses, it is the opinion of the authors that test measured data remains as a vital validation for model analysis predictions for complex and critical space structures. One may have attempted to justify proceeding without performing the ETM-3 modal survey due to the significant database of information from a similar design, namely the RSRM. However, nothing provides the assurance of accuracy for the prediction tools, as does actual test data. Some parameters simply cannot be obtained via any other methods, such as damping. In the subject study, all previous results indicated that the first axial mode would have significantly higher damping than observed in the modal test data. This parameter alone was a critical parameter in assuring accurate predictions for transient response of ETM-3 in the T-97 test stand. Although design loads were not exceeded when this knowledge was implemented, similar such findings have potential to result in exceedences of developed loads. This is especially true when design margins are forced to be tight and performance requirements prevent the luxury of over design.

Future Work

For over a decade, assumptions for appropriate values of solid rocket motor dynamic modulus have conflicted with those obtained from relaxation testing and Rheometric Dynamic Spectrometer test data due to modal response measured data findings. The ETM-3 modal test data provided valuable insights into further validating these historical assumptions as the indications of the first shell modes were consistent with previous assumptions. This discrepancy between these observations and traditional measurement method results has led to further study via modal test methods. Planning for detailed testing and analysis of a single motor segment is currently in work. This study is intended to significantly expand the previous single segment work using more refined methods of test and analysis. Answers will provide additional confidence in understanding appropriate methods of representing a viscoelastic material such as solid rocket motor propellant in tractable transient analyses. Complex modal analysis provides an option for handling such materials, but presents inherent problems with readily performed coupled loads analyses.

Further correlation of the FEM to the observed modal test data is also in work, particularly for the higher order combined bending and nozzle participation modes, and the post-burn modal survey results. Further modal frequency and potential mode shape optimization is planned. Additional knowledge gained in these activities will be used to augment the current RSRM program finite element model prediction capabilities.

REFERENCES

1) Mason, D. R., Morstadt, R. A., et al. "Pressure Oscillations and Structural Vibrations in Space Shuttle RSRM and ETM-3," 40th AIAA/ASME/SAE/ASEE Joint Propulsion Conference and Exhibit, Fort Lauderdale, FL, 2004.
2) "Final Report for Solid Rocket Motor DM-3 Modal Survey Ground Test," Structural Dynamics Research Corporation, San Diego, Ca., December 1978.
3) "Final Report for Solid Rocket Motor RM-1 Modal Survey Ground Test," ATK Thiokol Report, 1989.
4) Kammer, D. C, Mason, D. R., et al. "Test-Analysis Correlation of the Space Shuttle Solid Rocket Motor Center Segment," Journal of Spacecraft, Vol. 26, No. 4.
5) Kammer, D. C., "Optimal Placement of Triaxial Accelerometers for Modal Vibration Tests," submitted for publication to Mechanical Systems and Signal Processing, January 2001.
6) Peck, J., Torres, I., "A DMAP Program for the Selection of Accelerometer Locations in MSC/NASTRAN," 45th AIAA/ASME/ASCE/AHS/ASC Structures, Structural Dynamics and Materials Conference, Palm Springs, Ca., 2004
7) RSRM-DEV-03-036, "ETM-3 in T-97, Pre-fire Modal Survey Test Report", NASA/MSFC ED27 Report, October 2003
8) RSRM-DEV-03-037, "ETM-3 in T-97, Post-fire Modal Survey Test Report," NASA/MSFC ED27 Report, December 2003